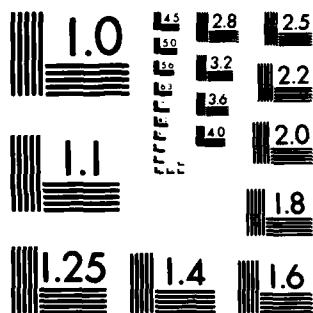END
DATE
FILMED

9 84

DTIC

MICROCOPY RESOLUTION TEST CHART
NATIONAL BUREAU OF STANDARDS-1963-A

AFGL-TR-84-0095

LWIR SIGNATURE FROM EXCEDE SPECTRAL

Fritz Bien

Space Dynamics Laboratories
Utah State University
Logan, UT 84322

Scientific Report No. 3

7 March 1984

Approved for Public Release; Distrubution Unlimited

DTIC
ELECTE
AUG 9 1984

B

AIR FORCE GEOPHYSICS LABORATORY,
AIR FORCE SYSTEMS COMMAND
UNITED STATES AIR FORCE
HANSCOM AIR FORCE BASE
MASSACHUSETTS 01731

84 08 09 070

This report has been reviewed by the ESD Public Affairs Office (PA) and is releasable to the National Technical Information Service (NTIS).

This technical report has been reviewed and is approved for publication

FRANCIS X. ROBERT
Contract Manager

RANDALL E. MURPHY
Branch Chief

FOR THE COMMANDER

RANDALL E. MURPHY
Acting Director
Infrared Technology Division

REPORT DOCUMENTATION PAGE

1a. REPORT SECURITY CLASSIFICATION Unclassified		1b. RESTRICTIVE MARKINGS None			
2a. SECURITY CLASSIFICATION AUTHORITY		3. DISTRIBUTION/AVAILABILITY OF REPORT Approved for Public Release; Distribution Unlimited			
2b. DECLASSIFICATION/DOWNGRADING SCHEDULE					
4. PERFORMING ORGANIZATION REPORT NUMBER(S) SDL/84-013 SSI-TR-42		5. MONITORING ORGANIZATION REPORT NUMBER(S) AFGL-TR-84-0095			
6a. NAME OF PERFORMING ORGANIZATION Spectral Sciences Inc	6b. OFFICE SYMBOL (If applicable)	7a. NAME OF MONITORING ORGANIZATION Contract and Grant Office Utah State University			
6c. ADDRESS (City, State and ZIP Code) 111 South Bedford St. Burlington MA 01803		7b. ADDRESS (City, State and ZIP Code) UMC 41 Logan UT 84322			
8a. NAME OF FUNDING/SPONSORING ORGANIZATION Air Force Geophysics Lab	8b. OFFICE SYMBOL (If applicable) LSP	9. PROCUREMENT INSTRUMENT IDENTIFICATION NUMBER F19628-83-C-0056 *Teradyne Research*			
8c. ADDRESS (City, State and ZIP Code) Hanscom AFB, MA 01731 F. X. Robert/Monitor		10. SOURCE OF FUNDING NOS.			
		PROGRAM ELEMENT NO. 62101F	PROJECT NO. 7670	TASK NO. 10	WORK UNIT NO. AK
11. TITLE (Include Security Classification) LWIR Signature From Excede Spectral					

12. PERSONAL AUTHOR(S)
Bien, F.

13a. TYPE OF REPORT Scientific No. 3	13b. TIME COVERED FROM 1/1/83 TO 9/30/83	14. DATE OF REPORT (Yr., Mo., Day) 1984 March 7	15. PAGE COUNT 42

16. SUPPLEMENTARY NOTATION
The work reported herein was perfromed under subcontract 83-031 to Space Dynamics Laboratories, Utah State University.

17. COSATI CODES			18. SUBJECT TERMS (Continue on reverse if necessary and identify by block number)
FIELD	GROUP	SUB. GR.	

19. ABSTRACT (Continue on reverse if necessary and identify by block number)

EXCEDE/SPECTRAL was launched from Poker Flat Research Range, Alaska, on 19 October 1979. This report presents selected LWIR data obtained both during electron gun operation and non-operation. It presents a simplified outgassing model and discusses $CO_2(v_2)$ emissions measured.

20. DISTRIBUTION/AVAILABILITY OF ABSTRACT UNCLASSIFIED/UNLIMITED ☒ SAME AS RPT. ☐ DTIC USERS ☐	21. ABSTRACT SECURITY CLASSIFICATION Unclassified	
22a. NAME OF RESPONSIBLE INDIVIDUAL Francis X. Robert/Contract Monitor	22b. TELEPHONE NUMBER (Include Area Code) 617/861-3641	22c. OFFICE SYMBOL LSP

DD FORM 1473, 83 APR   EDITION OF 1 JAN 73 IS OBSOLETE.

11. This title is UNCLASSIFIED.

TABLE OF CONTENTS

DTIC
ELECTE
AUG 9 1984
B

Accession For
NTIS GRA&I   ☑
DTIC TAR   ☐
Unannounced   ☐
Justification

By
Distribution/
Availability Codes
         Avail and/or
Dist   Special
A-1

DTIC
COPY
INSPECTED

LIST OF ILLUSTRATIONS

1. INTRODUCTION

The long wave infrared has received considerable attention recently due to development of instruments which operate well in this region. One of the great unknowns has been the effects of an electron excitation on the atmosphere, such as auroral activity, and what, if any, radiation may result.

Project EXCEDE is a DNA/AFGL experimental program designed to study the radiative processes in the atmosphere by exciting it with electrons from a rocketborne platform. The latest flight of this series, EXCEDE SPECTRAL,[1] contained a liquid helium cooled Circular Variable Filter Spectrometer (LiHe CVF) which measured the emissions from the atmosphere between 12 and 22 μm, both with and without electron dosing. This paper presents an analysis of these signals.

EXCEDE SPECTRAL was launched 19 October 1979 at 05:46:40 UT from Poker Flats, Alaska in a south to north trajectory along the geomagnetic declination as shown in Fig. 1. The conditions of the atmosphere were clear, dark, and aurorally quiet. It attained an apogee of 128.2 km which occurred 188 seconds after launch. Its nominal horizontal velocity was 330 m/s. The instrument package was despun after nosecone ejection with its long dimension elevated to an angle of approximately 43°. The electron beam pulsing sequence began at 115 km on the upleg and continued through until instrument separation at 72 km on the downleg. Not all of the electron guns worked at all times. The majority of the "beam on" data were taken when only gun 4

---

[1] "EXCEDE SPECTRAL Preliminary Results," R. R. O'Neil, editor, Air Force Geophysics Laboratory, Hanscom AFB, MA, Technical Memoradum No. 41, 1980.

EXCEDE: SPECTRAL

LAUNCHED 19 OCT 1979
POKER FLAT, ALASKA
5700 POUND PAYLOAD

ELECTRON ACCELERATOR
20-70 kW; 3 kV

OPTICAL / IR SENSORS
ROCKET BORNE
GROUND BASED

APOGEE 128 km

INITIAL BEAM
PULSE 115 km

FINAL BEAM
PULSE 72 km
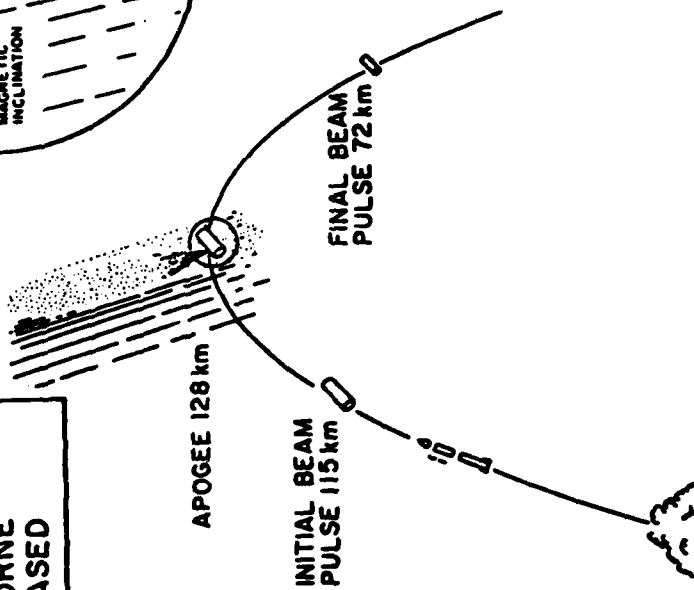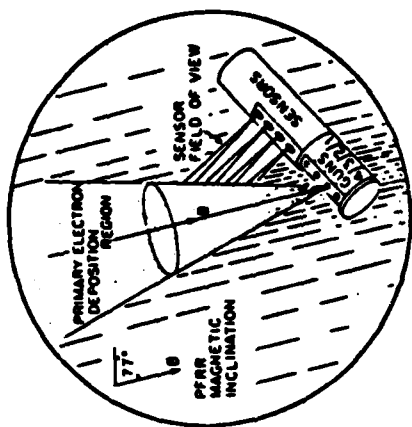
SPECTRAL MEASUREMENTS
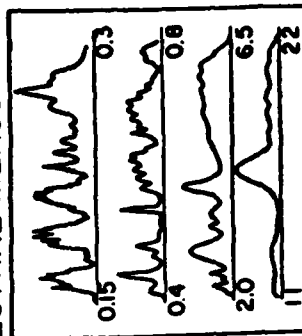
WAVELENGTH (microns)

Figure 1. EXCEDE/Spectral Flight Profile

was in operation. During a portion of the downleg, all four guns came on, providing much higher dose rates than in the other portions of the trajectory.

The payload onboard the vehicle is illustrated in Fig. 2. It contained 4 electron accelerators, capable of producing nominally 120 kW at 3 kV, and actually producing as much as 70 kW at 3 kV. The instrument package contained an array of ultraviolet, visible, and infrared spectrometers, photometers, and radiometers and both film and television cameras. Among the infrared instrumentation, there was an SWIR interferometer and CVF and a liquid He cooled CVF having three segments, a 180° segment operating between 3 and 7 μm, and 90° segments operating between 12 and 17 μm, and between 18 and 22 μm.

Next to the CVF is a bank of radiometers with filter wavelengths to measure N_2^+ first negative. These radiometers measured the amount of prompt emission from direct electron excitation of the atmosphere. There were blind spots between 16.8 and 17.8 μm and between 7 and 12.5 μm. The nominal bandpass of this instrument was 4% FWHM. The scan time of this instrument was 1.2 seconds, 0.6 seconds in the MWIR and 0.6 seconds in the LWIR. The instrument started operation 40.7 seconds after launch, and took continuous data until 321 sec after launch. A total of 232 scans were taken, of which 77 scans had at least some electron beam activity. The other scans surveyed the undosed atmosphere which included water outgassing, vehicle control jet emissions, and the natural background. Several scans in the initial part of the flight measured the reflection of the instrument cover, and other portions of the vehicle as they passed out of view of the detector.

VIEWING AFT

180

90 —

0 deg.

Q Probe 180
SC Probe 319 & 180
PF Probe 226
Main Door
Gyro Zoro Ref.
Launch Lug
All Optical Instruments
E Guns

Forward

(Major Axis)

Payload
(Side View)
All Instrument
View ⊥ to Major
axis except as
notes.

TALOS CASTOR
A51.970
EXCEDE II
(Spectral)

Recovery

ACS

Despin

TM

UV Diodes (1&2)

Cameras (B&W & Color)
    15 deg. aft of ⊥
TV Camera
Helium Spectrometer
Nitrogen Radiometer
Nitrogen Spectrometer
Photometers (8)
Nitrogen Interferometer
UV Spectrometer
Variable Spectrometer

E Gun (Master)

E Gun (Slave 1)

E Gun (Slave 2)

E Gun (Slave 3)
    All E Guns 30 Deg.
    Forward of ⊥

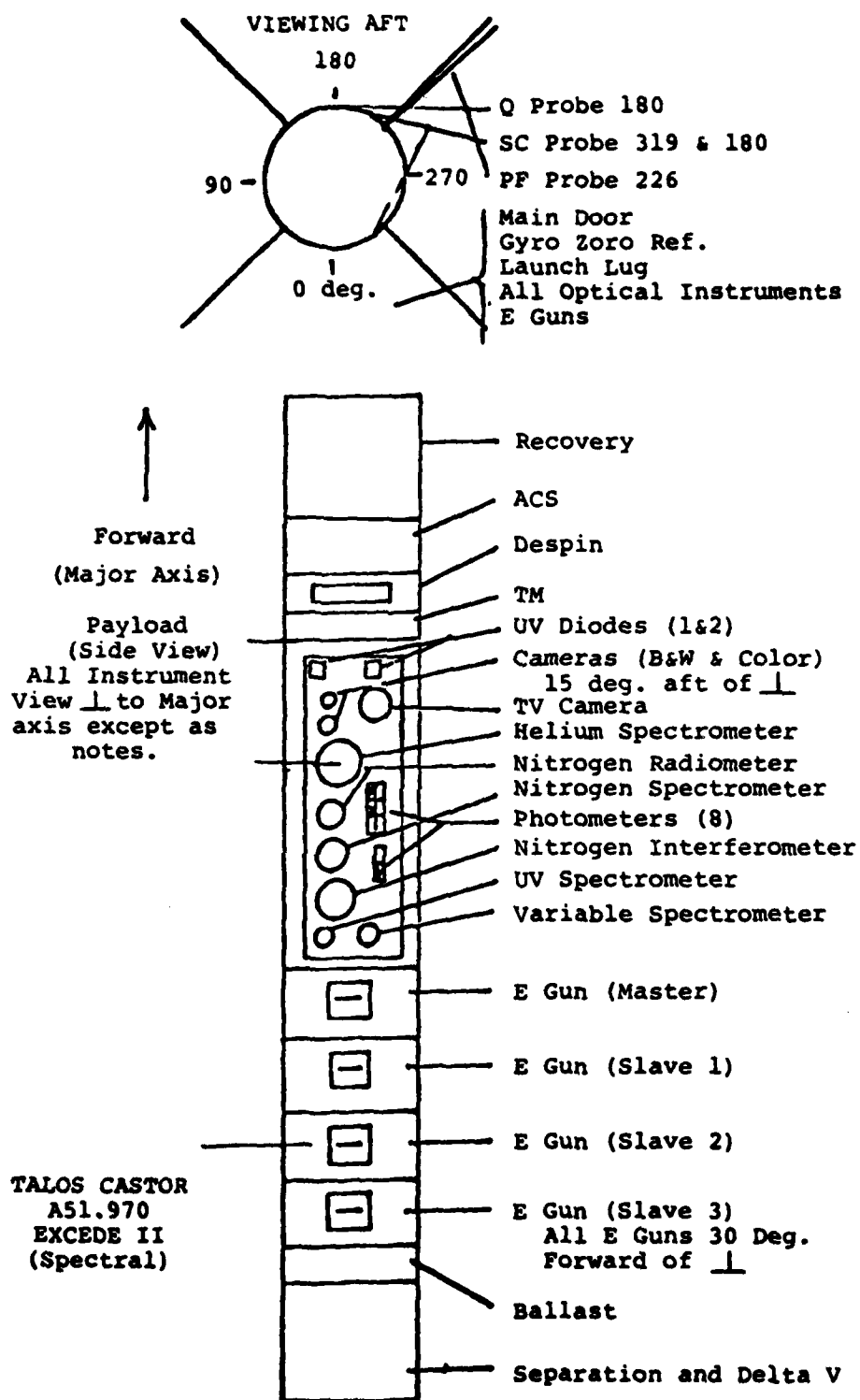Ballast

Separation and Delta V

Figure 2. Payload Instrumentation

4

2. DATA BASE

The CVF spectral data were taken in the form of an optical chopped signal which was telemetered digitally and retrieved using phase sensitive techniques. The original data set, reduced by using a digital clock, was presented in Report No. AFGL-TR-81-0224 in 1981.[2] This data showed a 40 Hz ripple, due to a slight non-synchronization of the digital clock and the CVF chopper frequency. This ripple was since removed using a specially designed digital filtering technique. In addition, some anomolies to the original calibration appeared, and were accounted for by applying corrections to the reduced spectral data. The revised CVF data, used in this report, was presented by Foley et al. (1982) in a special interim report by Boston College.[3]

Typical data, presented in this report, is shown in Fig. 3, beam off at 220 seconds after launch at 123 km altitude on the downleg, and Fig. 4, one electron gun on, 222 seconds after launch and 122 km altitude on the downleg.

The spectral features which were above the noise in Fig. 3 consist of 5.3 μm, due to NO, the 6.28 μm valley and the P and R branches due to H_2O, a 15 μm feature due to CO_2, a 16.2 μm feature

[2] "Analysis of Project EXCEDE II Circular Variable Filter Spectrometer Data," W. F. Grieder and C. I. Foley, Air Force Geophysics Laboratory, Hanscom AFB, MA, Rept. No. AFGL-TR-81-0224 (1981).

[3] "Analysis of Project EXCEDE II Circular Variable Filter Spectrometer Data Supplement I," C. I. Foley, W. F. Grieder, and N. Grossbard, Space Data Analysis Laboratory, Boston College (1982).
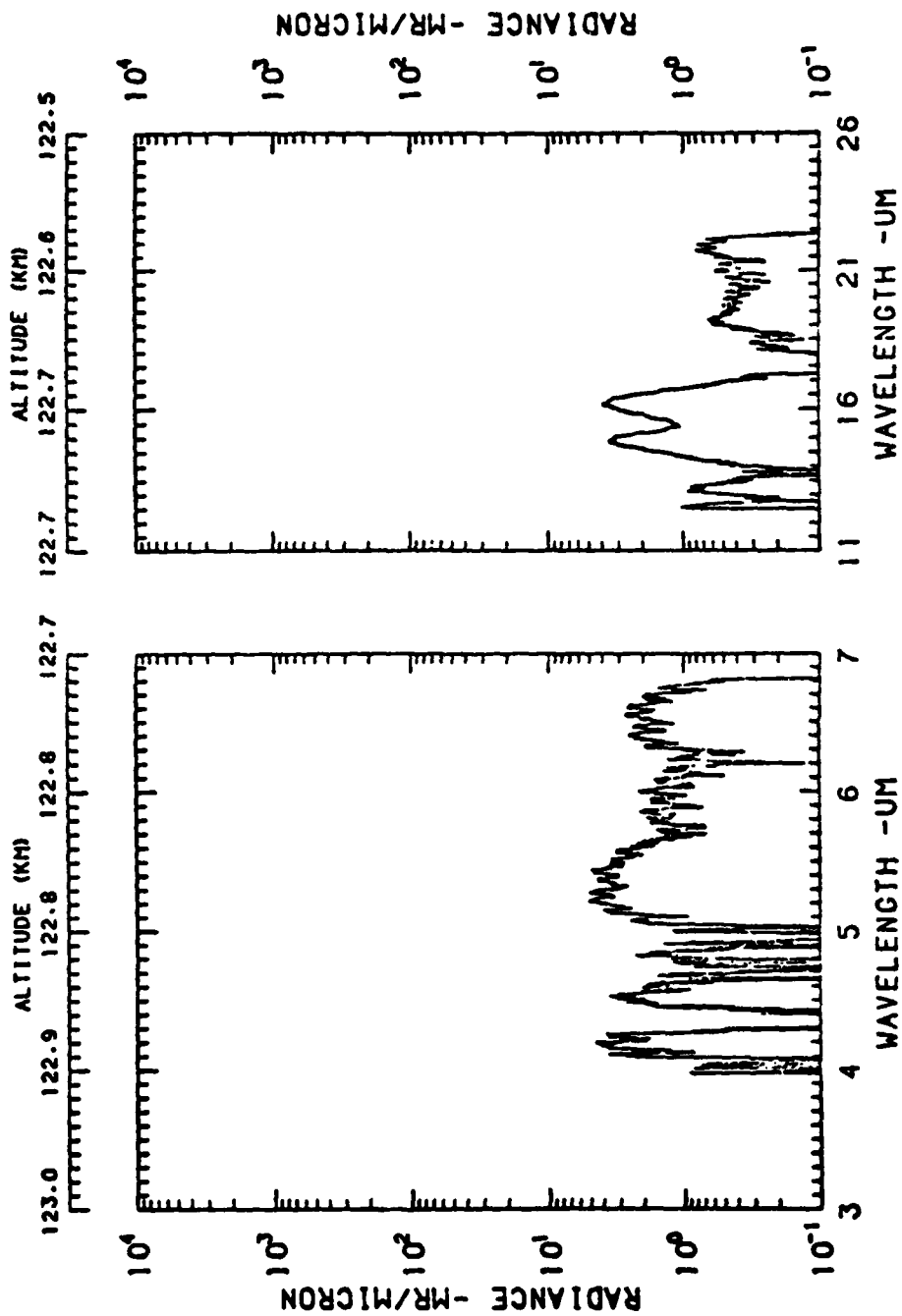
Figure 3. EXCEDE SPECTRAL Scan 1150, TAL = 220.4, ALT = 122.9, Filter = 119. Beam Off Data From 223 km Downleg. Between 4 and 7 μm Note NO at 5.3 and H_2O at 6.3 μm.
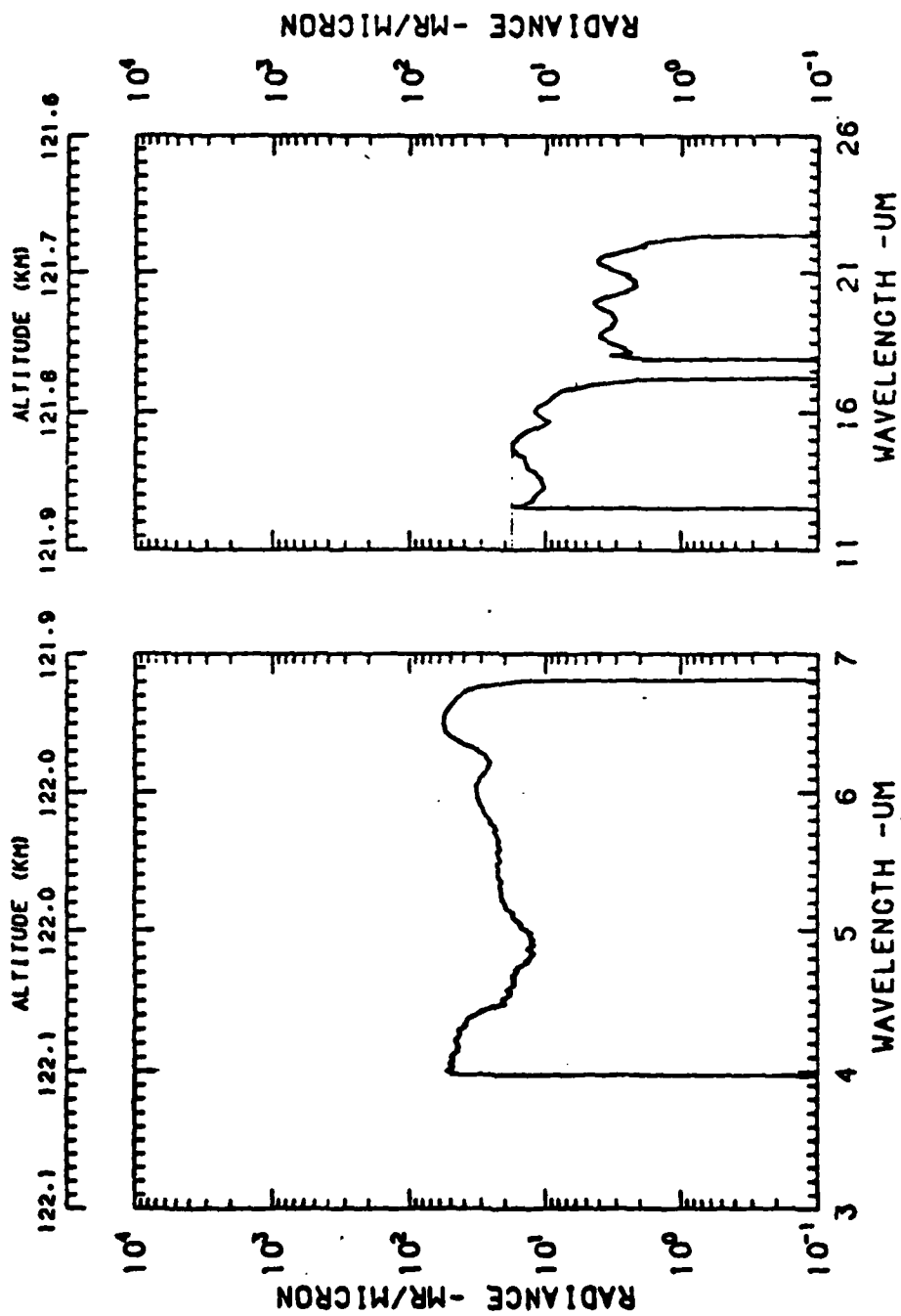
Figure 4. EXCEDE SPECTRAL Scan 1152 Electron Gun 4 Operating,
TAL = 222.888, ALT = 122.1, Filter 119.

due presumably to a surface contaminant and the features between 18 and 22 µm due to water vapor. Note that the instrument is more sensitive at longer wavelengths, therefore, the signal appears more distinguishable from the instrument noise.

Figure 3 shows the CVF signature with the beam on. There appears to be a slight hint of $CO_2(v_3)$ emission, a peak at 4.7 µm, possibly due to CO, NO at 5.3 µm is merged into H_2O at 6.2 µm. In the long wavelength portion, there seems to be an initial transient which is much narrower than the instrument function at 12.5 µm. Peaks at 14.5 µm, 15 µm and 16.2 µm are due to $CO_2(v_2)$ and the outgassing feature, lying above an OH rotational spectrum. The OH rotational spectrum is shown by the 18.6, 20 and 21.4 µm peaks.

In addition to the CVF spectra shown, a total of 230 other scans were made. Of particular value were scans with the instrument cover on, during the early portion of the flight, as shown in Fig. 5. These scans provided post flight calibration of the data which was not otherwise available, as the instrument was not recovered. The beam operation was correlated with the spectral scans to assess the effects of time dependence in the electron excitation of the atmosphere. It was found that all enhancements due to the electron excitation were fast with respect to the rise time of the instrument, thus, the signal rise was used, instead, as a correlator to relate the two different timing circuits used by the electron gun and the CVF.

Data was also taken after the instrument payload was separated from the electron gun module at 70 km on the downleg. These data were particularly useful in providing unambiguous peaks for CO_2, CO, and H_2O. These data were then used to ascertain spectral locations of emission features at higher altitudes.
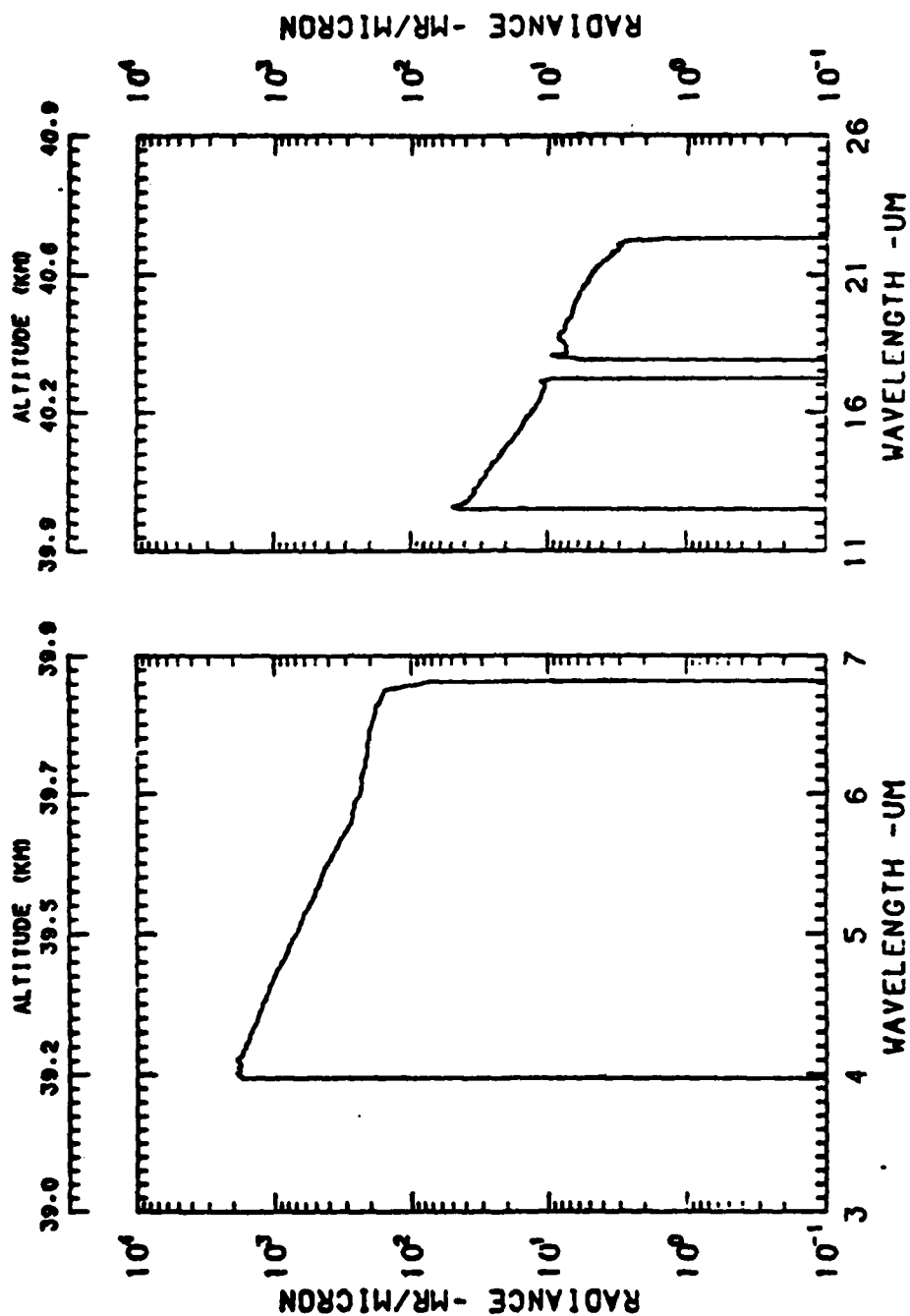
Figure 5. EXCEDE SPECTRAL Scan 1009, TAL = 50.3, ALT = 39.1, Filter 119. Cover on Data, Showing Instrument Response to Calibration Lamp After Normalization.

9

Data used in addition to these provided by the LiHe CVF
in this analysis include those taken from the 391.4 nm photom-
eters, the electron beam current monitors, and the UV spectrom-
eter. A typical pulsing sequence of the electron guns is shown
in Fig. 6. Shown here is the time sequence between 200 and 250
seconds and the current output of the four electron guns over
that period. We see that gun 4, which produced an average of
6 amperes, operated most consistently, while gun 3 produced up-
wards of 10 amperes with much shorter pulses. Gun 1 appeared
to arc and did not achieve sustained operation until later in
the flight. Gun 2 came into operation only twice during the
flight.
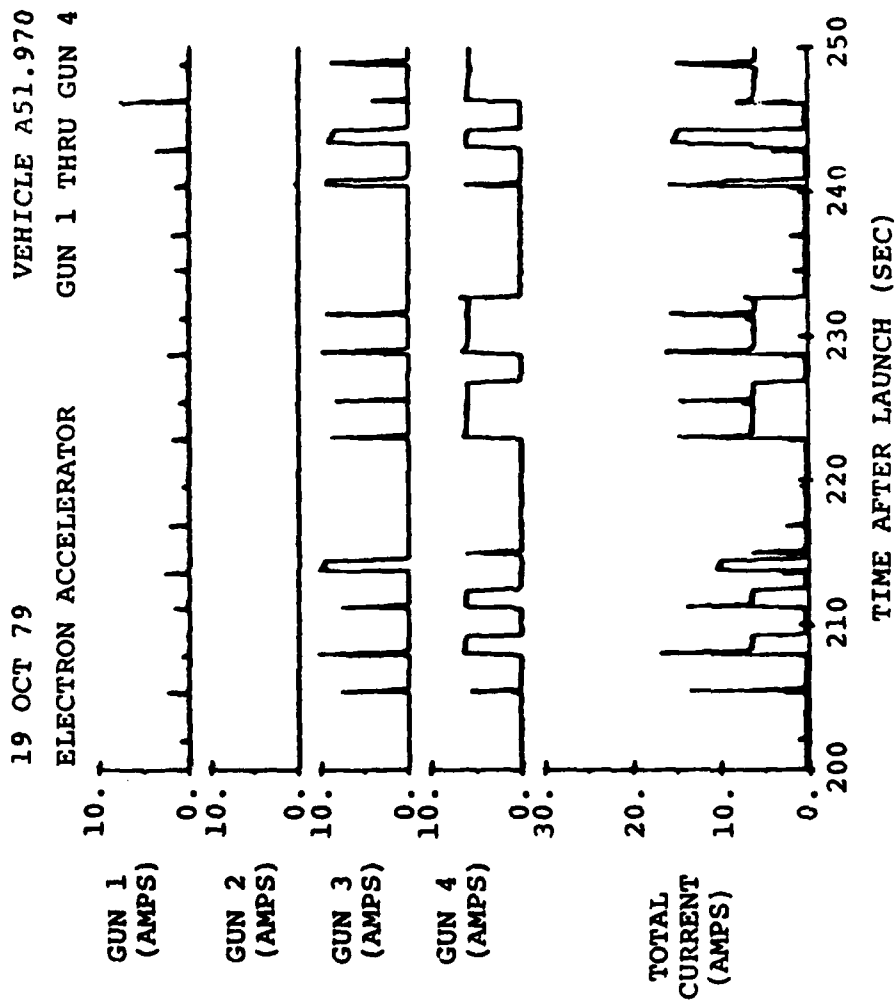
Figure 6. Gun Pulsing Sequence Between 200 and 250 Seconds After Launch. Gun 1 Was nearest Detectors.

11

3. BEAM OFF H₂O FEATURES

There were several distinct, identifiable features in the Li He CVF data with the electron beam off. Between 3.5 and 7 μm, we saw NO and $H_2O(\nu_2)$. Between 12 and 22 μm, there was $CO_2(\nu_2)$, a 16.2 μm contaminant, and water rotation between 18 and 22 μm. Because of the very unambiguous water signature both at 6.3 μm and between 18 and 22 μm, we are able to back out both the temperature and column density of the H_2O with a minimum of assumptions. Once this contribution to the overall signature is accounted for, the other emitters, CO_2, NO and possibly CO could be observed.

Water was observed not only by this instrument, but also by a Liquid N_2 cooled CVF and the SWIR interferometer. Water derivatives, OH and H, were observed during beam on data to be discussed in the next section. We deal here with deriving a temperature and column density for H_2O.

The CVF data from 18 to 22 μm matches the spectra of H_2O rotation at a temperature of 296°K, used in HITRAN (McClatchey, et al., 1973),[4] as is shown in Fig. 7 by the dashed curve. An actual rotational temperature cannot be assigned to the H_2O spectra, however, because of its relative insensitivity to temperature, as illustrated by the derived spectra for 500°K H_2O.[5] Since the same instrument recorded $H_2O(\nu_2)$ emission,

---

[4] "AFCRL Atmospheric Absorption Line Parameters Compilation," R. A. McClatchy, et al., Air Force Geophysics Laboratory, Hanscom AFB, MA, Rept. No. AFCRL-TR-73-0096, January 1973.

[5] "Exponential Wide Band Parameters For The Pure Rotational Band of Water Vapor," A. T. Modak, JQSRT 21, 131 (1979).
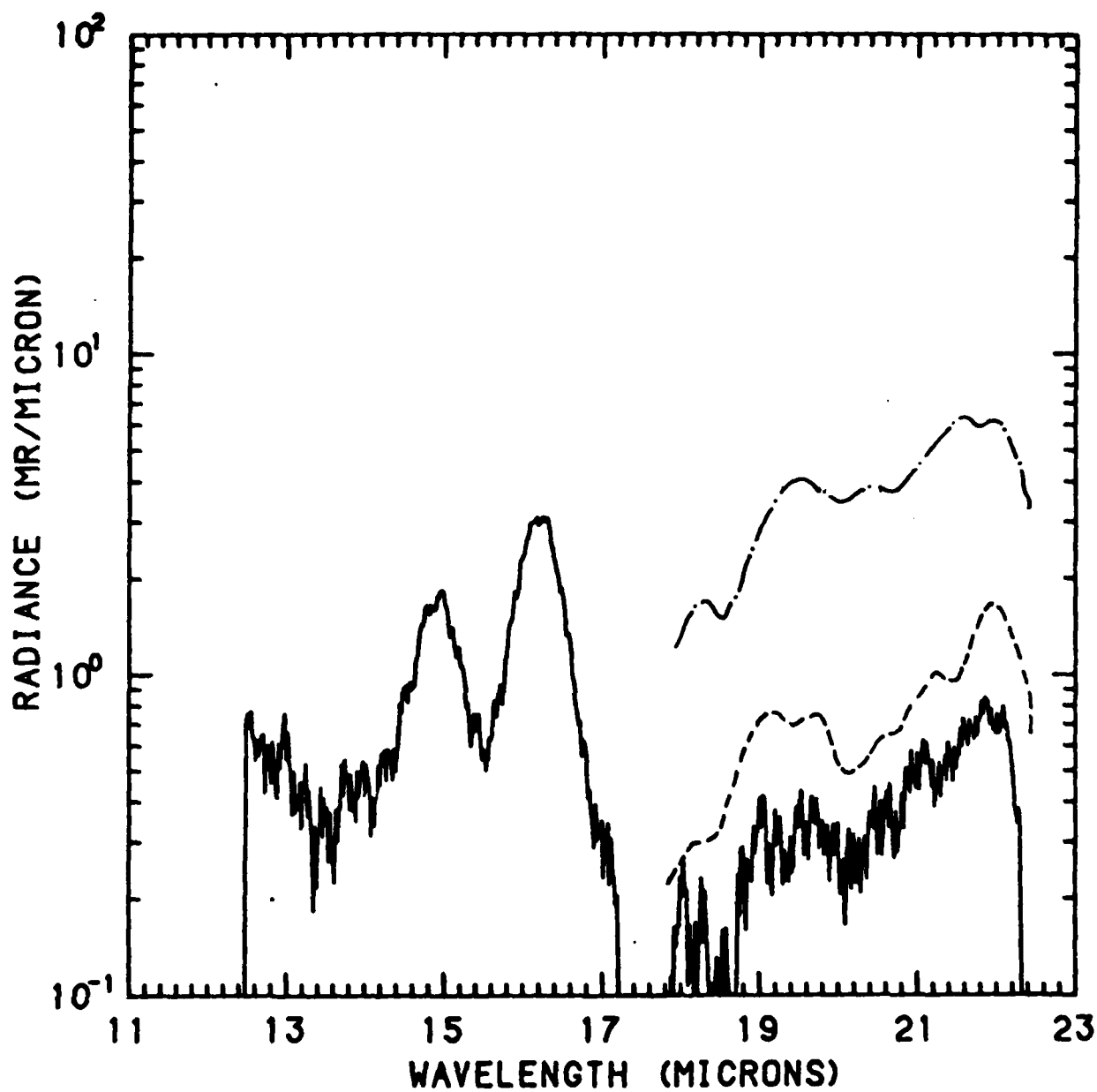
EXCEDE SPECTRAL SCAN 1133

Figure 7.   Comparison of 17 to 22 μm Emission With H_2O
            Rotational Spectrum. Dashed Lines Represent
            H_2O at 296°K From HITRAN, Dot Dash Represent
            H_2O From 500°K. The Curves are Separated
            For Clarity.

13

by assuming equilibrium, we can ratio this emission to the
water rotational emission to provide a characteristic H_2O vibra-
tional temperature.

It is important to operate in an uncontaminated portion of
the spectrum. Thus, for the 6.3 μm ν_2 band of H_2O, we use the
unambiguous peak at 6.55 μm during beam off operation. While
the location of the peak is a weak function of temperature, its
height is a function of both temperature and concentration.
Using absorption coefficients measured at low resolution, (Slack
and Ludwig, 1978)[6] we may calculate the emission intensity
from Kirchoff's law:

$$I = \epsilon R^O = R^O(1 - r) \tag{1}$$

where ϵ is the emissivity of the gas, r its reflectivity and
R^O the Planck blackbody function:

$$R^O d\lambda = \frac{2\pi c \omega^4 d\lambda}{\left[\exp(hc\omega/kT) - 1\right]}$$

$$= \frac{1.88 \times 10^{-5} \omega^4}{\left[\exp(hc\omega/kT) - 1\right]} \ d\lambda \quad MR/\mu m \quad . \tag{2}$$

Here, ω is the frequency of the radiation in cm^{-1}, T is the
temperature in ^OK, and hc/k is the second radiation constant
equal to 1.4388 cm^OK. The absorption for 300^OK water at the
Peak R branch region is 1.65 cm^{-1} at STP (Slack and Ludwig, 1978).
This converts to an absorption cross-section of

---

[6] "Plume Data Analysis of Advanced Propellants," M. Slack and
C. Ludwig, Air Force Rocket Propulsion Laboratory, Edwards AFB,
CA, Rept. No. AFRPL-TR-78-4, September 1978.

$$\sigma = k/N_{H_2O} = 1.65 \left(\frac{1}{2.69 \times 10^{19}} \right) \tag{3}$$

$$\sigma = 6.1 \times 10^{-20} \text{ cm}^2 \quad .$$

In the optically thin limit, the intensity from H_2O ν_2 in the R branch peak is thus

$$I_{6.5} = \frac{6.2 \times 10^{-12} \text{ N}\ell}{\exp(2230/T) - 1} \quad (MR/\mu m) \tag{4}$$

where $N\ell$ is the column density of H_2O in cm^{-2}.

The emission at 21.9 µm from water vapor is due to H_2O rotational emission lines within the 4% bandpass of the CVF. The major contributor to this feature is a single rotational line, 9,2,7 - 8,1,8 at 457.76 cm^{-1}. The sum of the integrated absorption coefficients weighted by the instrument function is 7.2×10^{-20} cm^{-1} molecule^{-1} at 296°K, or $\sigma = 4.2 \times 10^{-21}$ cm^2. This emission is primarily from high lying rotational lines of H_2O, having lower state energies of 586 cm^{-1} and greater, and heavily weighted at low temperatures by the 9,2,7 - 8,1,8 line having a lower state energy of 744 cm^{-1}.[4] A first order correction for this absorption coefficient with temperature is

$$\sigma_T = \sigma_{296} \left(\frac{1.10 \times 10^4}{T} \right) \exp(-1070/T) \quad . \tag{5}$$

The intensity from the 21.9 µm feature is thus

$$I_{21.9} = \frac{3.8 \times 10^{-11} \exp(-1070/T)}{T \left[\exp(658/T) - 1 \right]} \quad N\ell \quad (MR/\mu m) \tag{6}$$

The ratio of emission from 6.5 µm and from 21.9 µm is independent of the water column density in the optically thin limit; for low temperatures $(T << 2200°K)$

$$\frac{I_{6.55}}{I_{21.9}} = \frac{\left[.160T \exp(658/T) - 1\right]}{\exp(1160/T)} \tag{7}$$

Equation (7) is only a function of temperature.

From Eq. (7), the temperature of H_2O causing the emission was found to vary from $360^{\circ}K$ at the early portion of the flight, cooling to $200^{\circ}K$ near apogee, and increasing again as the vehicle returns to lower altitudes. This temperature history is shown in Fig. 8. The lower temperature limit is thought to be governed by the cooling of the water layer by boil-off until the heat of vaporization is equal to the heat input from the vehicle surface. As the surface water (ice) cools, it gives off heat until the heat flux into the ice balances the evaporation.

Since the vapor pressure is known for ice, we can calculate the effective column density of outgassing in two ways. The emission of H_2O ν_2 and rotation provides a column density of $1.5 \pm .5x10^{16}$ cm^{-2} 100 seconds after launch, dropping to $6 \pm 2x10^{15}$ cm^2 200 seconds after launch, and then dropping off as the vehicle returns to the atmosphere as shown in Fig. 9.

The scatter on the column measurements performed by substituting a temperature into Eq. (4) is large, as a small temperature change in the exponential term translates into a large variation in the calculated column density. Since the outgassing water vapor is not expected to be nonvarying over the 0.6 seconds between the measurement of the 6.5 μm ν_2 peak and the 21.9 μm rotational line peak, this translates into a large scatter in the column calculation. The drop-off in water concentration after 200 seconds after launch can be explained in several ways. After 200 seconds, the electron guns work at a higher duty cycle. Not only that, but gun 1 comes into operation. This causes the surface of the vehicle near the LiHe CVF to become hotter,
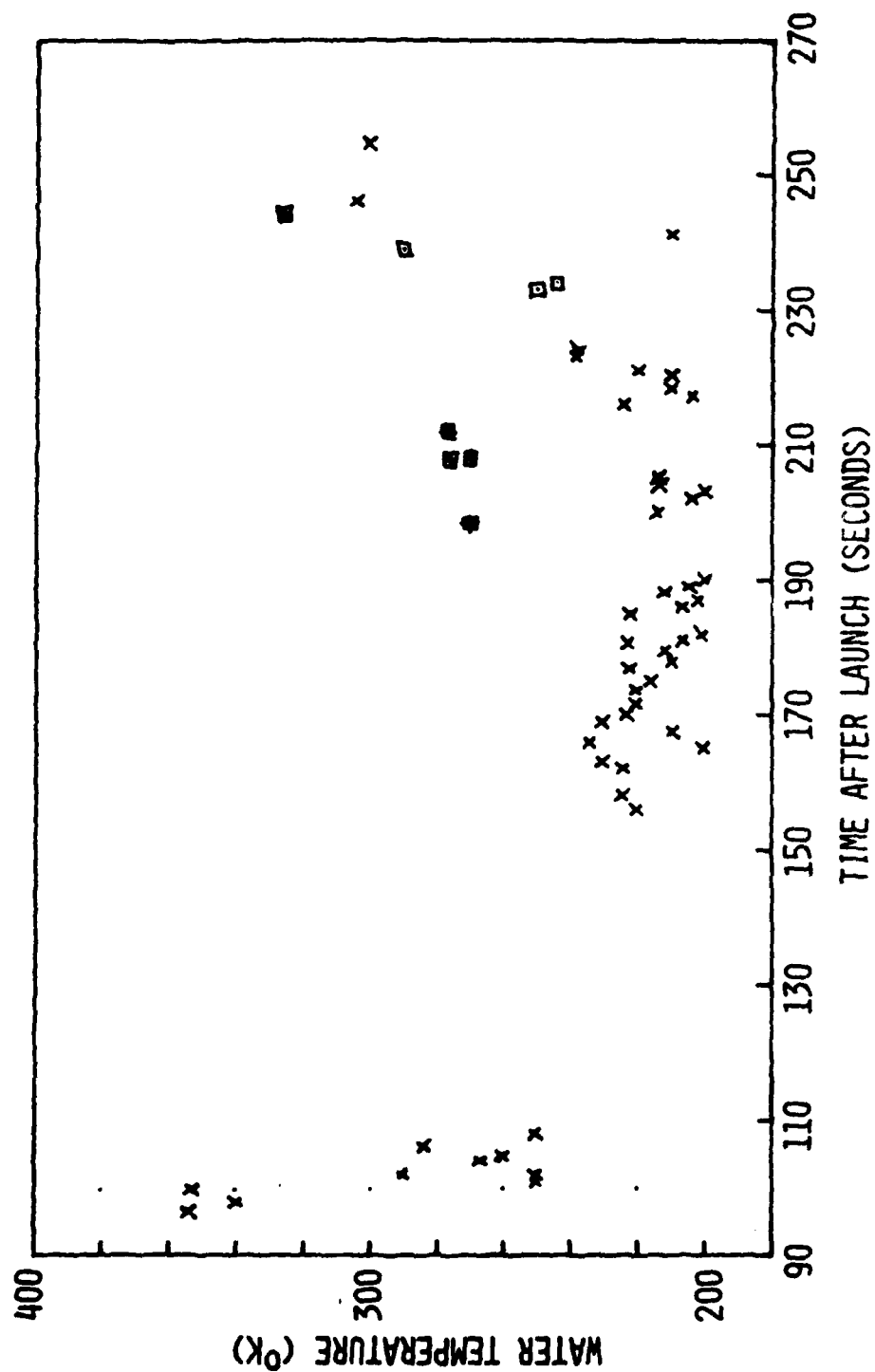
Figure 8. Temperatures Obtained by The Ratio of 6.5 μm R Branch ν_2 to 21.9 μm Rotational Line of H_2O. Squares Represent Data Taken Within One Second of Electron Beam Termination.
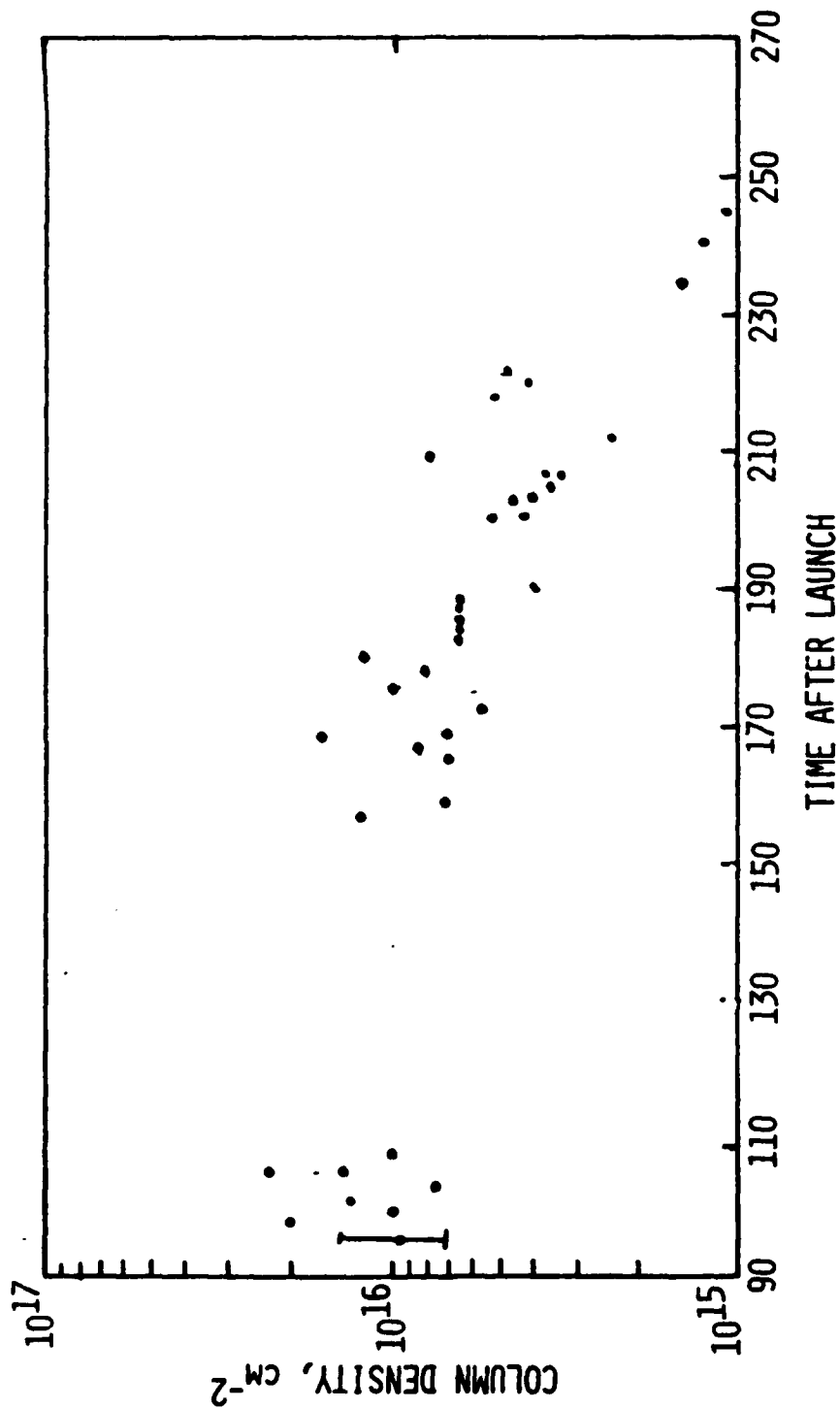
17

Figure 9. Column Density of H_2O as Derived From The H_2O ν_2 Emission and its Ratio to 21.9 μm H_2O Rotation.

therefore outgassing off the remaining ice. A second explana-
tion is that the ice has been nearly all evaporated, therefore
the temperature goes up as the insulating layer decreases.
Finally, all of the ice disappears as the water vapor temperature
increases, giving an increase in ν_2 emission, while the H_2O
rotational emission continues to decrease.

The water temperature also converts to a column density
from its vapor pressure. The characteristic dimension of the
vehicle times the density derived from the vapor pressure and
temperature gives a column density of

$$N\ell = \frac{pv}{RT}\ell = 3.54 \times 10^{16} \times .00105 \times \frac{273.16}{200}\ell$$

$$= 5.1 \times 10^{13} \, \ell cm^{-2} \quad .$$

(8)

From Eq. (8), one needs only the column length in order to
obtain the column density. This length must be on the order of
2 m in order to match the intensity ratio results, and is consis-
tent with the characteristic dimension of the vehicle. The vapor
pressure is a very strong function of temperature, however, as a
10 degree increase in temperature would correspond to 4 times the
vapor density. We thus have two ways of measuring column density,
each being a very strong function of temperature.

Thus, for the purposes of this analysis both methods for
determining the concentration appear consistent. This very large
vapor density has a number of implications. Since the amount of
outgassed water is proportional to the surface area, gas velocity
and density, the total water vapor leaving the vehicle during
the entire flight is

$$m = \dot{m}t = \rho Avt$$

(9)

for the 100 seconds in which the water vapor dropped to 1/3 of
its initial value, approximately 1.5×10^{20} molecules/cm^2 left the

vehicle skin. This corresponds to a layer 30 μm thick. If integrated over the entire vehicle skin, this would correspond to 2.3×10^{25} molecules, or about 650 g of water, or approximately 650 cm^3 of liquid water. Because of the viewing geometry of the LiHe CVF, looking into the wake of the vehicle, only 1/4 of the total surface would be necessary to contribute to the H_2O signature, hence only 170 g of water is necessary to explain the outgassing signature observed during the flight. We note that the amount of water observed is not inconsistent with quantities obtained by James[7] from analysis of the Hα feature during beam on conditions.

The temperature plot in Fig. 8 shows an increase (squares) of water temperature just after electron beam termination. This increase is similar to a "bake out" of surface water which one observes in the laboratory.

The amount of outgassed water, from this estimate, dominates the atmospheric species at the payload surface for all altitudes above 100 km. It is still comparable to the natural atmospheric concentration 1 m from the vehicle surface at 110 km. Water in this amount would dominate all atmospheric species within 10 meters of the vehicle at apogee. Reactions of H_2O + X are thus dominant reactions in the near field of the vehicle.

---

[7] "Preliminary Analysis of EXCEDE H_2O Spectral Emission Data," T. C. James, Lockheed Missiles & Space Co., Palo Alto, CA Rept. No. LMSC-D898458, December 1982.

4. BEAM ON H₂O FEATURES

A typical scan in the 12 to 22 μm region of the spectrum during electron beam operation is shown in Fig. 10. This figure is similar to Fig. 2, only enlarged to show the 18 to 22 μm region more clearly. Of particular interest is the three evenly spaced features between 18 and 22 μm. These peaks can be accounted for by line features convoluted with the CVF response. The valleys between the spectral peaks can nearly completely be accounted for by the CVF instrument spectral bandwidth. A synthetic spectrum of OH rotation,[8] if all states were emitting with the same band strength, is shown overlayed onto another such scan in Fig. 11. The valleys between the spectral peaks show some emission features which can be derived when the OH emission is subtracted from the synthetic spectrum. Each peak represents two very closely spaced rotation lines for the $X^2\Pi_i$ ground state of OH.[8] The spectra seem to show the uniform spacing of OH(R) plus spectral lines at 19.5 and 21 μm. While the intensities of these features are not accurately determined, they do show spectral shape, rather than an underlying continuum. These features will be discussed in further detail below.

The OH emission appears to be from the dissociative excitation of H₂O. Since the total column density of H₂O has been determined to approach 10^{16} cm^{-2}, it is not surprising that OH is

---

[8] "Spectral Line Parameters For The $A^2\Sigma$-X^2 (0,0) Band of OH For Atmospheric and High Temperatures," A. Goldman and J. R. Gillis, JQSRT 25, 111 (1981).

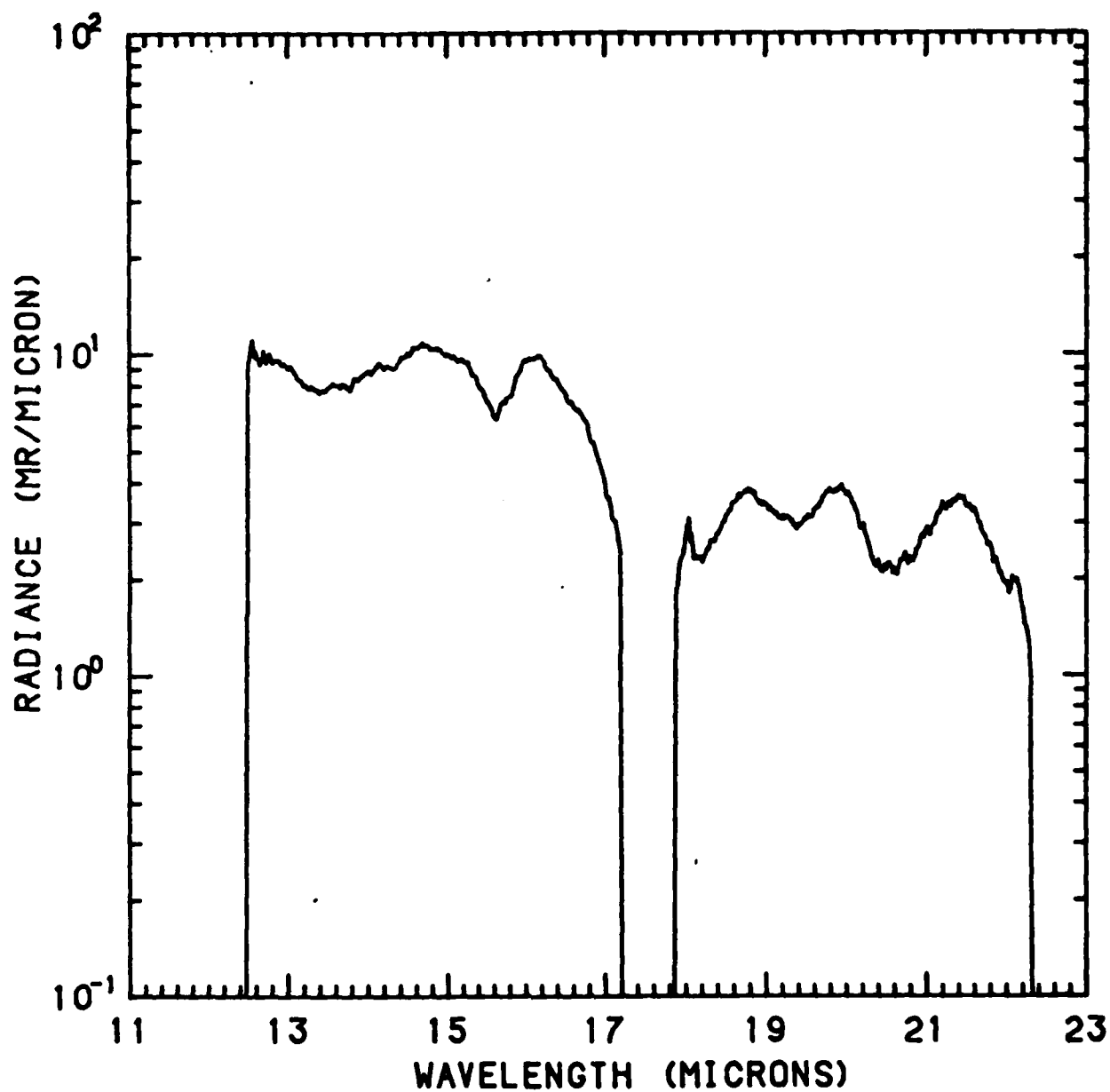Figure 10.   EXCEDE SPECTRAL Scan 1123 Taken at Apogee (188 sec
              after launch). Note the Regular Spectral Features
              Between 18 and 22 μm.
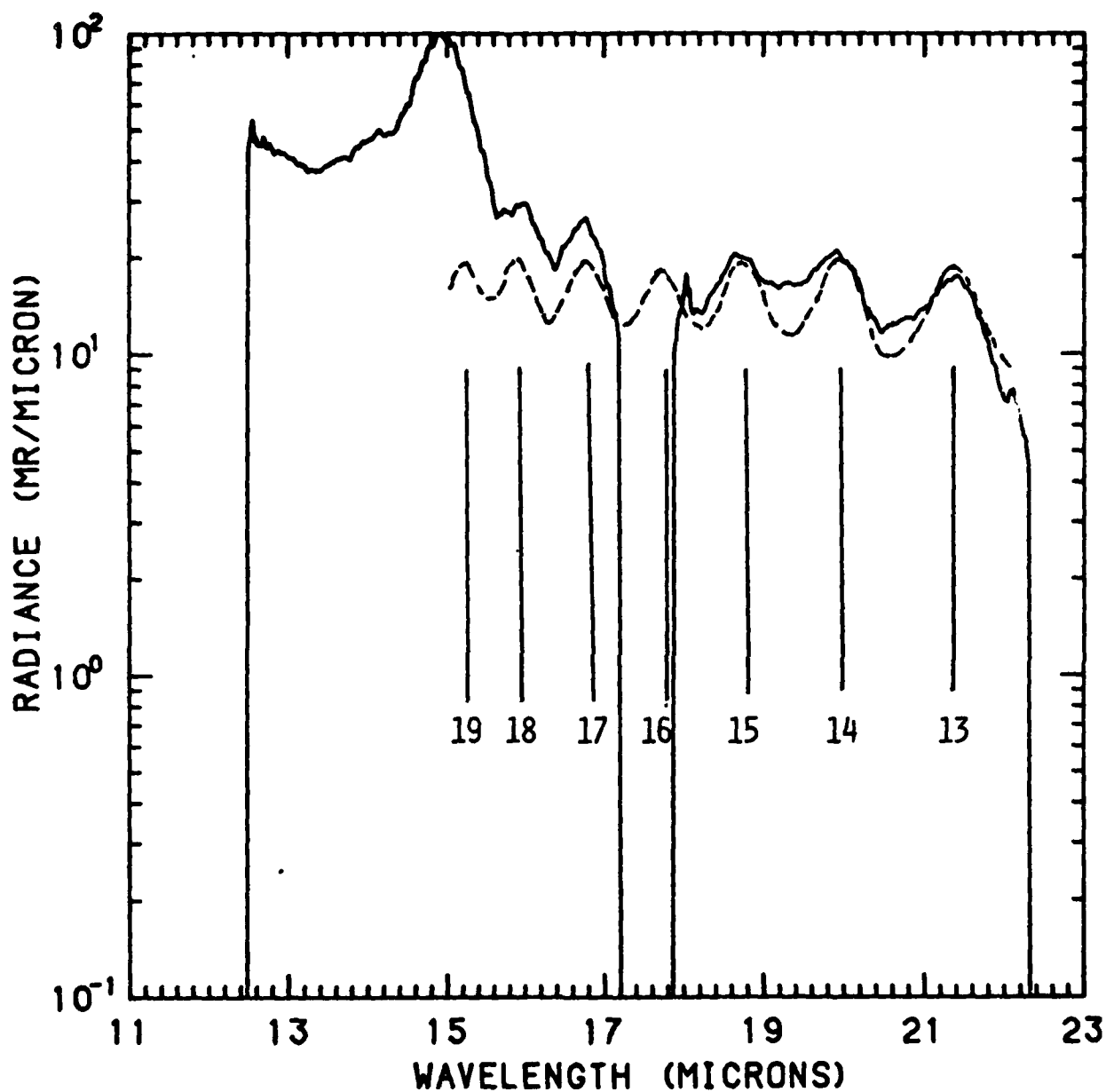
22

Figuve 11.   LWIR Portion of Scan 1185, 265 Seconds After Launch,
             101 km Altitude, Gun 3 on.   The Dashed Curve Shows
             The Synthetic Spectrum of OH Rotational Lines of
             Equal Intensity.

23

formed. The amount of OH formed should be proportional to the amount of H_2O in the excited column, times the efficiency of converting H_2O to OH by electron impact. Working backwards, the amount of emission of OH is known and if we assume classical lifetimes for OH emission, the radiative lifetimes scale as v^2, and are all less than 0.2 ms, thus, their emission is governed by their formation rate only. Since the emission of OH rotation is for $\Delta K = 1$, molecules formed in the upper rotation levels would cascade down the rotational ladder until they collide with other molecules and rotationally equilibrate.

The rotational peaks of OH are nearly uniform, suggesting that the OH is formed in a high rotational state and is cascading through the region where the emission is observed. Figure 11 shows the LWIR signature at 265 seconds after launch, or 101 km altitude downleg. We see that the spectra shows peaks corresponding to K = 18, 17, 15, 14 and 13. The peak at K = 13 may be lower due to quenching of this rotational level. It is interesting to note that the 16.2 µm feature, seen at higher altitudes, or earlier time, would lie between K = 17 and 18. This feature has all but disappeared at this altitude.

The rotationally hot OH can be ascribed to direct dissociative excitation of H_2O by electrons, as well as collisional quenching of vibrationally hot OH. High rotational states of OH has previously been observed in the OH laser transitions and found to be preferentially formed in the $K' = 12$, 13 for resonant transfer from $v' = 1$, and $K' = 19$, 20 for resonant transfer from $v' = 2$.[9,10] Collision frequencies of $H_2O + OH^{\dagger}$ are on the

[9] "The OH and OD Laser, Collisional-Induced Energy Transfer Pumping," J. W. Smith and D. W. Robinson, J. Chem. Phys. 68, 5474 (1978).

[10] "Vibrational-Rotational-Translational Energy Transfer in Ar + OH. Quasiclassical Trajectory State-to-State Cross Sections," D. L. Thompson, J. Phys. Chem. 86, 2538 (1982).

order of 10^{+3} sec^{-1} near the vehicle and would control the num-
ber of OH(R) formed in this manner. A column density of 10^{11} cm^{-2}
of OH (v=2) would be necessary to produce the OH(R) emission
signal of 10 MR/μm assuming v$\rightarrow$R transfer for OH(v) occurs one
out of every 10 collisions with H_2O. The vibrational lifetime
of (v=1) is 0.08 sec. A vibrational signal at 2.8 μm of 1.2 MR
should be detected when 10 MR of rotation is seen. In addition,
approximately 0.5 MR at 1.43 μm should be observed. Since these
rates are well within the 23 MR recorded in the 2.7 μm region,
attributed to the 10^{16} cm^{-2} H_2O, it is not inconceivable that OH
formed vibrationally hot can be quenched into one of the rota-
tional levels which is close in energy to produce the observed
emission, and yet the OH(v) be buried in the H_2O 2.7 μm signal.

If we assume a direct production scheme,[11]

$$e + H_2O \rightarrow OH(R) + H + e \qquad\qquad (10)$$

The intensity from OH(R) can be assumed to be governed by its
formation rate, as its radiative lifetime is shorter than 2×10^{-4}
seconds. The observed signature at apogee of 4 MR/μm, times the
instrument function of 0.72 μm gives 2.9 MR. Since the column
density of water vapor was determined to be about 10^{16} cm^{-2}
we can back out a production rate of k_e = 0.32 sec^{-1}. We can
compare this number to the 391.4 nm emission from N_2^+, 3.3 MR
over a column density of 1.66×10^{11} cm^{-3} and a column length of
60 m across the 30 meter cloud to get the ratio

$$\frac{\phi_{OH}}{\phi_{(N_2^+1-)}} = \frac{I_{OH}[N_2]\ell_{N_2}}{I_{391.4}[H_2O]\ell_{H_2O}} = \frac{2.9}{3.3} \frac{(1.66\times10^{11} \times 6\times10^3)}{10^{16}}$$

$$\qquad\qquad (11)$$

$$= 0.11$$

[11] "Electron Deposition in Water Vapor, With Atmospheric Appli-
cations," J. J. Olivero, R. W. Stagat, and A. E. S. Green,
J. Geophysical Res. 77, 4797 (1972).

Since the cross-section for 391.4 nm radiation has been well established,[12] we take this ratio and establish a relative efficiency, or effective cross-section:

$$\sigma_{OH} = \frac{\varphi_{OH}}{\phi_{3914}} \sigma_{3914} = 2.2 \times 10^{-18} \times 0.11 \tag{12}$$

$$= 2.7 \times 10^{-19} \text{ cm}^{-2} \quad .$$

We note that this derived cross section is approximately one half of the H_{α} cross-section used by Olivero et al.[11] This comparison, however, as pointed out by James,[7] is dubious without consideration of diffusion of the water cloud with respect to the vehicle. We address this in the next section.

The OH signature observed on EXCEDE: SPECTRAL has a number of important atmospheric implications in addition to merely the study of contamination. The natural atmosphere has a 10 ppm mixing ratio for H_2O at these altitudes therefore natural events would not produce detectable amounts of OH(R). However, in the case as heaved atmospheres, where water from lower altitudes is transported up, there can be large amounts of water vapor, and sufficient means to excite that vapor to produce detectable OH signals.

An estimate of the OH(R) contribution to a 50 kR(N_2^+1NEG) IBCII aurora is $0.11 \times \phi_{H_2O} \times 50kR = 0.05$ R. Nightglow of OH, on the other hand, shows a much larger contribution of OH(v) produced by $H + O_3$ at lower altitudes. Using the balloon

---

[12] "Cross Section for Electron-Impact Excitation of the (0,0) First Negative Band of N_2^+ from Threshold to 3 keV," W. L. Borst and E. C. Zipf, Physical Review A 1, 834 (1970).

measurements of the 8-6 band presented by Moreels et al. (1973)[13] and their subsequent model[14] we get OH(v=1) concentrations of 10^3 cm^{-3} at midnight at 80 km. Since this concentration is collisionally controlled at this altitude, the production of OH(R) and subsequent radiation is approximately

$$\frac{dOH(R)}{dt} = \frac{\left[OH(v)\right]}{\tau_0} = 3 \times 10^5 \text{ cm}^{-3} \text{ sec}^{-1} \tag{13}$$

wl.ere τ_0 is the quenching time of OH^*, assumed to be approximately 10^{-3} gas kinetic or, 10^{-2} sec. For a column height of 10 km, this would produce 30 kR of OH(R) signal, close to being measurable by many new instruments.

The OH(R) signature is thus seen to be possibly a very important emitter in the LWIR during manmade disturbances of the atmosphere, and be possibly detectable even during normal nightglow.

[13] "Balloon Observations of The 8-6 OH Band in The Day and Night Airglow," G. Moreels, A. V. Jones, and J. E. Blamont, Planet. Space Sci. 21, 1945 (1955).

[14] "An Oxygen-Hydrogen Atmospheric Model and Its Application to The OH Emission Problem," G. Moreels, G. Megie, A. V. Jones, and R. L. Gattinger, J. Atmospheric and Terrestrial Physics 39, 551 (1977).

5. SIMPLIFIED OUTGASSING MODEL

The actual observation of water vapor outgassing from the
payload is a complex problem involving position of the outgass-
ing source(s), vehicle velocity, temperature field of the payload,
and viewing geometry of the particular instrument which is used
to detect the outgassing. This problem is compounded by the
fact that the instrument field of view is weighted by the near-
field. For the basis of estimating the outgassing signature, we
make a number of simplifying assumptions, more to assess the
character of the outgassing than to come up with an accurate
predictive model.

From Fig. 1, it was seen that the payload is a long thin
cylinder, oriented at 43° with respect to the flow at apogee,
and passing at different aspects with respect to the flow
stream, through 90°, on the descent. The detectors of interest
are thus always looking through the wake of the vehicle. The
effects of this wake are more pronounced at low altitudes where
the interaction with atmospheric molecules occur within a few
tenths of a cm from the vehicle. At high altitudes, above 120
km, the water molecules must move several vehicle radii before
colliding with an atmospheric species. Thus, we may approximate
the outgassing as a free expansion into a vacuum. The effect of
vehicle motion is only to cause the collisions with atmospheric
species to be closer to the vehicle skin in the leading edge of
the payload and further away in the trailing edge. Thus, when
looking into the wake of the vehicle, a model of a freely expand-
ing gas wave, whose concentration varies with distance from the
source, should be good at distances near the vehicle. Far away
from the vehicle, this wake interacts with the atmosphere, and a

28

diffusion model would apply. At these long distances the vehicle can be treated as a point source.

In the near field, the vehicle acts as a cylindrical source where density of outgassants falls off as $1/r$. If we define a distance $\hat{r}$ as the distance from the vehicle in which the vehicle appears to become a point source, then at distances large compared to $\hat{r}$ the species concentration falls off as $1/r^2$ and is governed by diffusion, while at small distances with respect to $\hat{r}$, the species expands as $1/r$. We may approximate the near field as

$$n(r) = n_o a/r \qquad a \le r \le \hat{r} \qquad (14)$$

where n_o is the number density of outgassant at the surface of the vehicle of radius a. Thus, the total column density in the near field is

$$\int_a^{\hat{r}} n(r)dr = n_o a \ln(\hat{r}/a) \qquad (15)$$

and in the far field

$$n(r) = \int_{\hat{r}}^{\infty} n(r)dr = \int_{\hat{r}}^{\infty} n_o \frac{a\hat{r}}{r^2} dr = n_o a \ . \qquad (16)$$

The total column density is thus

$$N\ell = n_o a \left[1 + \ln \frac{\hat{r}}{a}\right] \ . \qquad (17)$$

Using 6 m as the characteristic length $\hat{r}$, with the 0.4 m vehicle radius, the column length becomes 1.5 meters, consistent with the beam off observations discussed in Section 2. Note that $N\ell$ is not a sensitive function of what value we choose for $\hat{r}$. The model is then of water in the solid state, on the surface

of the vehicle, boiling off at a vapor pressure corresponding to the surface temperature of 200°K, and expanding as $1/r$ away from the vehicle for the first 6 meters and as $1/r^2$ out to infinity. The electron beam impacts the water a distance 2 m away from the vehicle to a distance of 6 m from the vehicle with primary unscattered electrons, and from the surface on out with scattered primaries as well as hot secondaries. The vapor pressure of water is much higher than that of the natural atmosphere near apogee, so that collisions with the atmosphere play only a minor roll in perturbing the outgassing signature.

From this simplified model, the water column density in the vicinity of the $N_2^+(1-)$ emission should be approximately 30% of the total water column density, implying that the OH(R) cross-section in Eq. (12) is a factor of 3 higher, or about 9×10^{-18} cm^2.

6. $CO_2(\nu_2)$ EMISSION

The 15 μm feature of CO_2 was seen both in beam on and beam off conditions and was preliminarily analyzed by us.[1] This signature is being reanalyzed using the updated calibrations. Using these new calibrations, together with the already identified OH spectra, the actual contributions from CO_2 ν_2 can be assessed. This is illustrated in Fig. 12. While this subtraction was performed by hand, a finer meshed subtraction of the entire data base is currently being programmed. The locations of various combination bands, written as ν_1, ν_2, ℓ, ν_3, and the Fermi resonance term, can be seen from the subtracted shape. The two spectral features at 19.2 and 21 μm are from the residues left after convoluting the CVF instrument function with the OH line locations.

While Fig. 12 can only be analyzed qualitatively, since the relative emission rates of K = 19 vs K = 13, 14, 15 of OH is not known, we note that the hot bands of CO_2 are excited by the electron beam. These hot bands all have radiative lifetimes much shorter than the fundamental, thus could provide the enhancements observed at 15 μm. These bands also explain the increase in spectral width as observed at higher altitudes, shown in Fig. 13, reproduced from Ref. (1). As the instrument descends into the atmosphere, the natural emission from hot bands of CO_2 rise as does the fundamental, as would be expected from the increasing CO_2 density. Below 105 km, the center of the fundamental becomes self-absorbed, leading to the apparent increase in natural hot band emission. Since the emission from the $CO_2(\nu_2)$ with beam on also shows the enhanced hot band
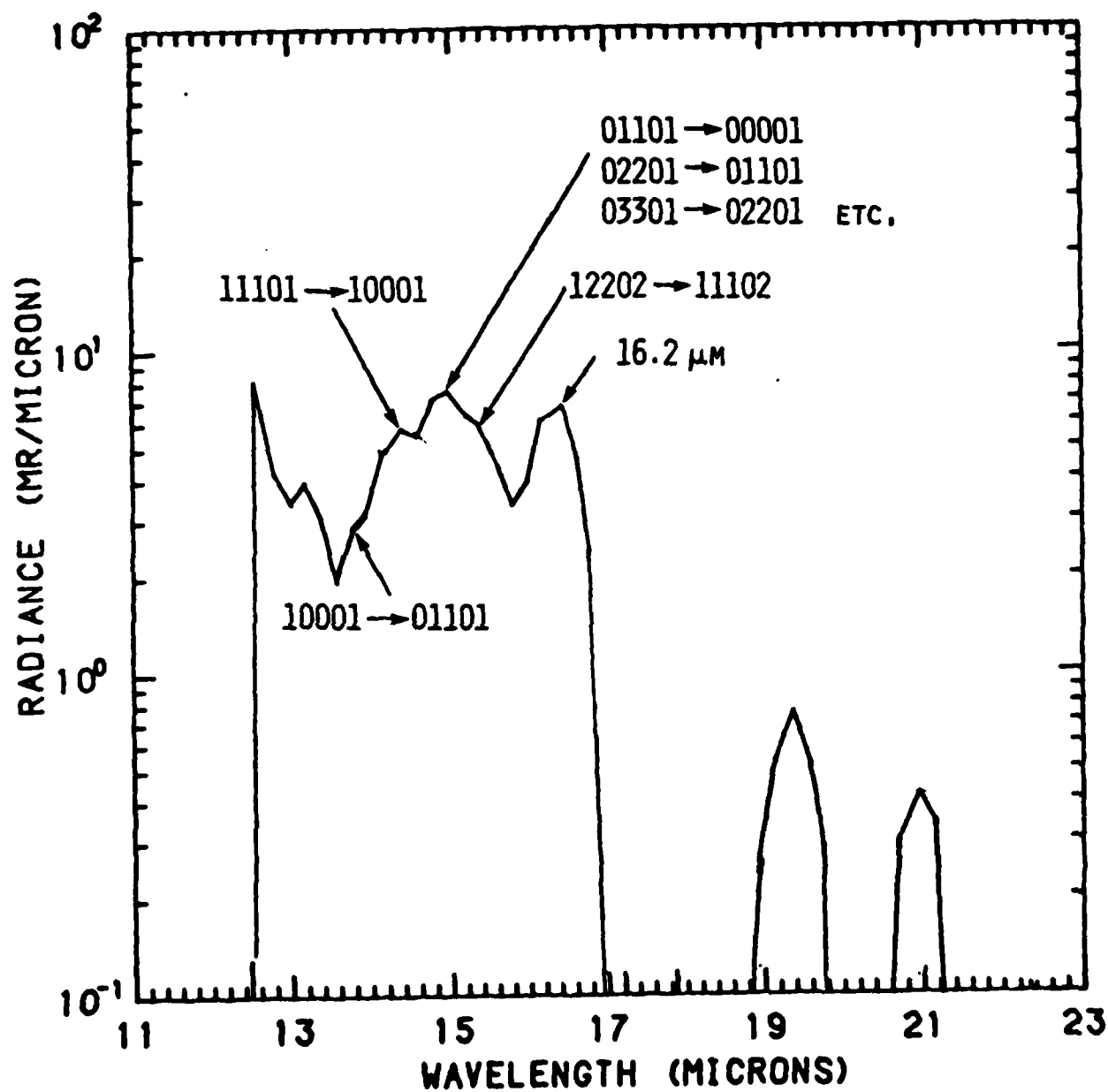
31

Figure 12. Spectral Scan 1124 (apogee) After OH (K=13→19) was
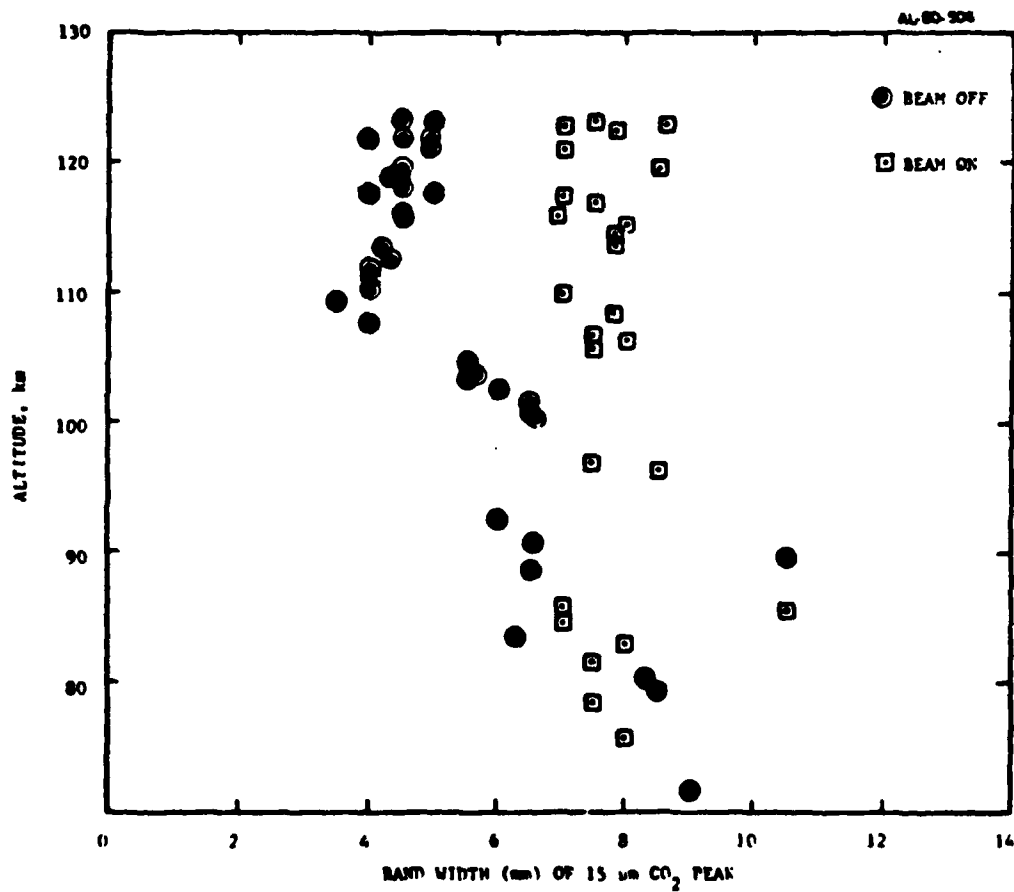Subtracted. Numbers Represent $CO_2 \nu_2$ Band Locations
Using McClatchey Notation.

32

Figure 13. Bandwidth of $CO_2(\nu_2)$ Band as a Function of Altitude
for Both Beam On and Beam Off Conditions. Note
Relative Constant Bandwidth During Beam On and
Variation With Altitude During Beam Off.

emission, the increase in emission with electron dosing may still be present. However, the self-absorbed background emission would mask these signals.

While the complete data base obtained in EXCEDE Spectral must be analyzed, and contributions of OH rotational emissions assessed, higher spectral resolution data is also necessary to give further insight on emissions from "hot" bands. It is expected that these hot band emissions would behave in a non-thermal way during electron excitation.

7. CONCLUSIONS

The majority of the emission seen in EXCEDE Spectral in the 12 to 22 μm region was from H_2O, which produced OH when bombarded by electrons. This H_2O was found to contribute 90% of the molecules within 1 cm of the vehicle skin at apogee. The water cloud can be pictured as vapor boiling off the skin and moving several meters before being brought to rest in the atmosphere. While the expanding cloud appears to be a major source of radiation, it does not comprise a large amount of water on the skin of the vehicle, averaging a layer 30 μm thick over the outer surface.

Even though the contamination by water vapor dominated the LWIR signals measured on EXCEDE Spectral, several things have been learned. The $CO_2(\nu_2)$ signature seems to be enhanced by electron beam excitation. This data needs further analysis for definitive rates and excitation mechanisms. The water itself provided useful information in the formation of OH(R). These signatures showed a mechanism for a possibly important source of nuclear induced emission, both from H_2O carried up in a heaved atmosphere and from missile trails which deposit very large amounts of water vapor. The rocket plume-nuclear interaction is perhaps one of the most important sources of LWIR interferences which would be encountered when using long wavelength detectors in a nuclear environment. Even though the radiant intensity of the H_2O rotation is low, its interaction with electrons would provide orders of magnetude increases in signature. Since these sources would have spatial character, they may prove formidable interferents.

The emission from OH(R) may occur when OH(v) is collisionally quenched into OH(R). This v-r transfer, responsible for the OH laser transitions, may be an important source of LWIR emission in the atmosphere.

8. REFERENCES

1. "EXCEDE SPECTRAL Preliminary Results," R. R. O'Neil, Editor, Air Force Geophysics Laboratory, Hanscom AFB, MA, Technical Memorandum No. 41, 1980.

2. "Analysis of Project EXCEDE II Circular Variable Filter Spectrometer Data," W. F. Grieder and C. I. Foley, Air Force Geophysics Laboratory, Hanscom AFB, MA, Rept. No. AFGL-TR-81-0224 (1981) , AD A 109894

3. "Analysis of Project EXCEDE II Circular Variable Filter Spectrometer Data Supplement I," C. I. Foley, W. F. Grieder, and N. Grossbard, Space Data Analysis Laboratory, Boston College, MA (1982). AFGL-TR-81-0224, AD A109894.

4. "AFCRL Atmospheric Absorption Line Parameters Compilation," R. A. McClatchey, et al., Air Force Geophysics Laboratory, Hanscom AFB, MA, Rept. No. AFCRL-TR-73-0096, January 1973, AD762904

5. "Exponential Wide Band Parameters For The Pure Rotational Band of Water Vapor," A. T. Modak, JQSRT 21, 131 (1979).

6. "Plume Data Analysis of Advanced Propellants," M. Slack and C. Ludwig, Air Force Rocket Propulsion Laboratory, Edwards AFB, CA, Rept. No. AFRPL-TR-78-4, September 1978.

7. "Preliminary Analysis of EXCEDE H_2O Spectral Emission Data," T. C. James, Lockheed Missiles & Space Co., Palo Alto, CA, Rept. No. LMSC-D898458, December 1982.

8. "Spectral Line Parameters for The $A^2\Sigma-\chi^2$ (0,0) Band of OH For Atmospheric and High Temperatures," A. Goldman and J. R. Gillis, JQSRT 25, 111 (1981).

9. "The OH and OD Laser, Collisional-Induced Energy Transfer Pumping," J. W. Smith and D. W. Robinson, J. Chem. Phys. 68, 5474 (1978).

10. "Vibrational-Rotational-Translational Energy Transfer in Ar + OH. Quasiclassical Trajectory State-to-State Cross Sections," D. L. Thompson, J. Phys. Chem. 86, 2538 (1982).

DATE
ILME